Diffusion on fractals

Ben O'Shaughnessy

Department of Chemical Physics, The Weizmann Institute of Science, 76100 Rehovot, Israel

Itamar Procaccia*

Department of Chemistry and The James Franck Institute, The University of Chicago, Chicago, Illinois 60637

The issue of diffusion on fractals is addressed with stress on the question of how to generalize the diffusion equation for Euclidean lattices to the case of fractal lattices. Such an equation is proposed on the basis of scaling arguments. The solutions of this equation are interpreted as analytic envelopes of the exact probability distribution $P(r,t)$ which is far from smooth. In fact it is shown that $P(r,t)$ has discontinuities which appear self-similarly on all length scales. The exactly soluble examples of Sierpiński gaskets embedded in general dimension d are analyzed. The predictions of the diffusion equation (involving no free parameters) are in very close agreement with the results of numerical simulations. A renormalization-group theory for the Green's function is developed to support the diffusion equation and to shed light on the nonanalyticities in $P(r,t)$.

I. INTRODUCTION

The problem of diffusion on fractal structures[1] is closely related to other "linear" problems on fractals such as the Schrödinger equation,[2] the equation for mechanical vibrations,[3] the laws of electrical conductivity,[4] etc. A relation with the localization problem has also been suggested. Thus, besides being of intrinsic importance (e.g., interesting applications to transport in porous media[5] and percolation networks[6]) the study of diffusion on fractals sheds light on all these related problems as well. The aim of this paper is to present a theory of the probability distribution $P(\mathbf{r},t)$ for a random walker on a fractal lattice; in particular a generalization of the Fickian diffusion law for Euclidean lattices to fractal lattices is presented.[7] The equation is derived on the basis of scaling arguments, and is supported by a renormalization-group analysis and by numerical simulations on some simple fractals amenable to exact theory. For these examples, solutions of the diffusion equation are obtained with no free parameters; close agreement with numerical simulations is found.

The main results previously derived concerning dynamics and transport on fractals are briefly outlined in the following. Given a fractal of dimension D embedded in Euclidean space of dimension d, the mean-square displacement after time t of a random walker on the fractal obeys[1]

$$\langle r^2(t) \rangle \sim t^{2/(2+\theta)} , \tag{1.1}$$

where r is measured in the Euclidean space. The index θ is in general nonzero (in contrast to Euclidean lattices where $\theta=0$). Together with D it determines the scaling exponent for the conductivity (see below, Sec. III), and the density-of-states exponent[3,8] for small eigenvalues ϵ:

$$\rho(\epsilon) \sim \epsilon^x , \tag{1.2}$$

where $x = D/(2+\theta) - 1$. The "fracton" or "spectral" di-

mension $\tilde{d}$ is defined[3] by $\rho(\epsilon) \sim \epsilon^{\tilde{d}/2-1}$; it is the effective dimensionality of reciprocal space for a fractal (cf. $\rho \sim \epsilon^{d/2-1}$ for Euclidean lattices). From (1.2) one finds $\tilde{d} \equiv 2D/(2+\theta)$. The index θ arises also in the probability to return to the origin $P(0,t)$,

$$P(0,t) \sim t^{-D/(2+\theta)} \tag{1.3}$$

and other statistical properties such as the number of distinct sites visited.[3] The reason that D must be supplemented by θ to determine all these dynamical properties is that the latter depends on features of the topology of the fractals (such as connectivity, etc.) which are not in one-to-one correspondence with the mass scaling (as determined by D).

In the following we wish to go beyond these scaling laws to generate a theory for the probability density $P(r,t)$ where $P(r,t)dr$ is the probability per site that at time t the walker is in the shell between r and $r+dr$ around the origin. We shall show that $P(r,t)$ is highly nonanalytic, and in fact contains discontinuities on all length scales. However one can consider the envelope of this quantity, $\hat{P}(r,t)$, and argue that the dynamics of $\hat{P}(r,t)$ are well approximated by the differential equation[7]

$$\frac{\partial \hat{P}(r,t)}{\partial t} = \frac{1}{r^{D-1}} \frac{\partial}{\partial r} \left[Kr^{D-1-\theta} \frac{\partial \hat{P}(r,t)}{\partial t} \right] . \tag{1.4}$$

The envelope $\hat{P}(r,t)$ will be shown to be an excellent fit to $P(r,t)$. For the exactly soluble examples we calculate the number K, so that Eq. (1.4) contains no free parameters. The solution of Eq. (1.4) is

$$\hat{P}(r,t) = \frac{2+\theta}{\Gamma(D/(2+\theta))} \left[\frac{1}{K(2+\theta)^2 t} \right]^{D/(2+\theta)}$$
$$\times \exp \left[-\frac{r^{2+\theta}}{K(2+\theta)^2 t} \right] . \tag{1.5}$$

From this solution one finds immediately

$$\langle r^2(t)\rangle = [K(2+\theta)^2 t]^{2/(2+\theta)}$$

$$\times \Gamma((D+2)/(2+\theta))/\Gamma(D/(2+\theta)) \qquad (1.6)$$

and $\hat{P}(0,t)\sim t^{-D/(2+\theta)}$ in agreement with Eqs. (1.1) and (1.3). It is clear, however, that Eq. (1.5) contains much more information; this will be examined below.

The arguments for Eq. (1.4) are presented in Sec. II. In the same section we consider also the family of d-dimensional Sierpiński gaskets[9] for which we calculate the number K. The idea behind this calculation is a comparison of the steady-state currents predicted by Eq. (1.4) with a source at $r=0$ and sinks at the boundaries to a direct and exact calculation of the same currents. In Sec. III we present a renormalization-group theory for the Green's function. This theory is used to support the arguments of Sec. II and to shed light on the nonanalytic properties of $P(r,t)$. In Sec. IV we present a number of numerical simulations on d-dimensional Sierpiński gaskets. Comparisons of $\hat{P}(r,t)$ and $P(r,t)$ for $d=2,3,4$ are presented, as are plots to demonstrate the self-similar nature of the singularities in $P(r,t)$ on all the (available) length scales. The paper concludes with a discussion in Sec. V.

II. ANALOG OF FICKIAN DIFFUSION ON FRACTALS

In Euclidean spaces the probability distribution for a diffusing particle obeys the equation

$$\frac{\partial P(\mathbf{r},t)}{\partial t} = \hat{K}\nabla^2 P(\mathbf{r},t) , \qquad (2.1)$$

where $\hat{K}$ is the diffusion constant. For δ function initial conditions one can transform to spherical coordinates and integrate out the angular degrees of freedom. The resulting equation is

$$\frac{\partial P(r,t)}{\partial t} = \frac{K}{r^{d-1}}\frac{\partial}{\partial r}\left[r^{d-1}\frac{\partial P(r,t)}{\partial r}\right] , \qquad (2.2)$$

where all the constants have been absorbed in K. We turn now to the question as to what the analog of Eq. (2.2) for fractal lattices is.

A. Scaling argument

We shall consider an origin $r=0$ and hyperspherical shells of radius r in the embedding d-dimensional space. Let $M(r,t)dr$ be the probability to find a diffusing particle in the shell between r and $r+dr$. By conservation of probability

$$\frac{\partial M(r,t)}{\partial t} = \frac{\partial}{\partial r}J(r,t) , \qquad (2.3)$$

where $J(r,t)$ is the net radial current through the shell. Let us define the average probability density per site $P(r,t)$ by

$$M(r,t)=P(r,t)N(r) , \qquad (2.4)$$

where $N(r)$ is the number of sites belonging to the fractal in a shell at radius r, per unit shell thickness. To obtain a differential equation for $P(r,t)$ from (2.3) and (2.4) we require in addition a constitutive relation equating $J(r,t)$ with the gradient of $P(r,t)$ multiplied by a conductivity. However both the conductivity and $N(r)$ are not expected to depend smoothly on r for any lacunar fractal. In fact these are expected to fluctuate around a smooth scaling law with the fluctuations persisting on all length scales. In consequence we anticipate similarly singular behavior for $P(r,t)$ (as is borne out by numerical simulation in Sec. IV) whose gradients are therefore not defined. However, we propose that the usual such relations exist for $\hat{p}(r,t)$, the smoothed envelope of $p(r,t)$:

$$\hat{J}(r,t)=\hat{\sigma}(r)\frac{\partial\hat{p}(r,t)}{\partial r} , \qquad (2.5)$$

where $\hat{J}(r,t)$ and $\hat{\sigma}(r)$ are the *envelopes* of the current and conductivity, respectively. In general we expect dependences on the angular variables also to appear in (2.5): the right-hand side of (2.5) has been approximated by preaveraging over these variables. Thus $\hat{\sigma}(r)$ is the total conductivity at r (i.e., the integral of the radial conductivity over a shell), and the terms involving derivatives of the probability with respect to angular variables vanish due to the "spherically" symmetric initial conditions.

Just as we defined envelopes for J and σ, so we define $\hat{N}(r)$ and $\hat{M}(r,t)$ to be the envelope of $N(r)$ and $M(r,t)$, respectively. The envelope analog of Eqs. (2.3) and (2.4) are

$$\frac{\partial\hat{M}(r,t)}{\partial t} = \frac{\partial}{\partial r}\hat{J}(r,t) \qquad (2.6)$$

and

$$\hat{M}(r,t)=\hat{P}(r,t)\hat{N}(r) . \qquad (2.7)$$

Substituting Eqs. (2.5) and (2.7) in (2.6), we get

$$\frac{\partial\hat{P}(r,t)}{\partial t} = \hat{N}^{-1}(r)\frac{\partial}{\partial r}\left[\hat{\sigma}(r)\frac{\partial\hat{p}(r,t)}{\partial r}\right] . \qquad (2.8)$$

The smoothed $\hat{N}(r)$ is determined by requiring that the number of sites in a ball of radius L that belong to the fractal will equal L^D. This means that

$$\hat{N}(r)=Dr^{D-1} . \qquad (2.9)$$

Note that this equation implies an appropriate choice of the dimensionless variable r [i.e., $\int_0^L \hat{N}(r)dr = CL^D$ with $C=1$]. To smooth $\hat{\sigma}(r)$ we first define the conductivity per site by

$$\hat{\sigma}(r)=\hat{K}(r)\hat{N}(r) \qquad (2.10)$$

and recall the equivalence of the stationary electrical conductivity problem and the stationary diffusion problem. Fix a potential ϕ at the origin and a zero (ground) potential at the shell of radius r. The total integral resistance $R(r)=\phi/\hat{J}$. Let us now assume the smooth envelope of the resistance scales according to $\hat{R}(r)\sim r^\alpha$. Then the envelope $\hat{\sigma}(r)$ at the shell r is given by

$$\hat{\sigma}(r) \sim [\partial \hat{R}(r)/\partial r]^{-1} \sim r^{1-\alpha} . \tag{2.11}$$

A smooth $\hat{N}(r)$ and a smooth $\hat{\sigma}(r)$ imply a smooth $\hat{K}(r)$ which obeys

$$\hat{K}(r) \sim r^{2-\alpha-D} . \tag{2.12}$$

Denoting θ as

$$\theta \equiv D + \alpha - 2 , \tag{2.13}$$

we find finally

$$\hat{K}(r) = Kr^{-\theta} , \tag{2.14}$$

where K is a constant. Using (2.14), (2.10), and (2.9) in (2.8), we arrive at the desired equation (2.4). The solution (2.5) agrees with the form suggested in Ref. 10. Note that the index θ reflects the anomaly in conductivity which derives from the anomalous fashion in which conductors are combined to form a fractal lattice. For Euclidean lattices the conductivity σ scales with N where N is the number of conductors put together to form a shell. In the fractal lattice we put Dr^{D-1} conductors together but get

$$\sigma(r) \sim r^{-\theta} r^{D-1} \sim (r^{D-1})^{(D-1-\theta)/(D-1)} \tag{2.15}$$

or

$$\sigma \sim N^{(D-1-\theta)/(D-1)} . \tag{2.16}$$

In other words, on the fractal the conductors are put together such as to leave holes on all length scales; as a result the conductivity grows more slowly than N. We note that the index θ which reflects this anomaly is precisely the one responsible for anomalous diffusion, cf. Eq. (1.6). Indeed the scaling law (2.10) is the expression of this equivalence. The same law has been argued for in a different manner in Ref. 11, while a similar relationship is proposed in Ref. 12, involving the exponent which determines the scaling of the coupling constant rather than the resistance.

B. Determination of K

Once D and θ are known, the only quantity to be determined in Eq. (1.4) is K. We shall demonstrate its calculation for the Sierpiński gasket. The idea is to match the steady-state properties of Eq. (1.4) with an independent calculation of the steady-state properties of the gasket. The calculation can be done for the gaskets embedded in d dimensions. In the text we treat $d = 2$ and in Appendix A the case of general d.

1. Steady-state solutions of Eq. (1.4) for Sierpiński gaskets

Consider a gasket embedded in two dimensions as shown in Fig. 1, with a potential (source) ϕ at the top and zero potential (sinks) at the bottom. We seek the steady-state solution for $\hat{P}(r)$, which is found from

$$\frac{\partial}{\partial r} \left[Kr^{D-1-\theta} \frac{\partial \hat{P}(r)}{\partial r} \right] = 0 \tag{2.17}$$

subject to the boundary conditions $P(0) = \phi$, $P(r_0) = 0$.
The solution of Eq. (2.17) is
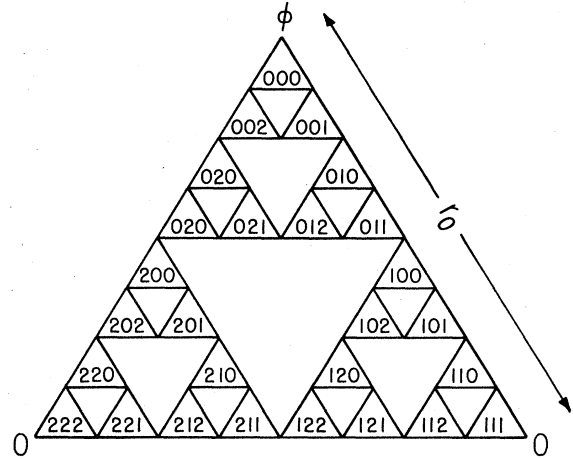
FIG. 1. The Sierpiński gasket and the coordinate system used in this paper. ϕ is a potential at the top triangle whereas zero is the potential at the bottom triangles. r_0 is the overall size of the gasket.

$$\hat{P}(r) = \phi \left[1 - \left[\frac{r}{r_0} \right]^{2+\theta-D} \right] . \tag{2.18}$$

To get the steady-state current we recall the basic equation (2.5) which together with (2.9), (2.10), and (2.14) implies that

$$\hat{J} = KDR^{D-1-\theta} \frac{\partial \hat{P}}{\partial r} . \tag{2.19}$$

Equation (2.18) in (2.19) leads therefore to

$$\hat{J} = -\phi KD(2+\theta-D)r_0^{D-\theta-2} . \tag{2.20}$$

2. Independent calculation of $\hat{J}$

To calculate the current $\hat{J}$ independently we have to introduce a coordinate system for the gasket which facilitates analysis.[13] In a gasket with 3^n triangles, *the triangles are labeled by* $i = \sum_{k=0}^{n-1} a_k 3^k$, $a_k = 0,1,2$, see Fig. 1. Given the inner length scale, the diffusion occurs by hopping from site to site with a diffusion equation $1/W\dot{Q}_p = -4Q_p + \sum_q Q_q$ where Q_p is the probability to be in the site p and the q runs over four nearest-neighbor sites . W is the conductance of a bond. By summing over the three vertices that belong to a given triangle we can derive the equivalent equation in the triangle representation

$$P_i = W \left[\sum_j P_j - 3P_i \right] . \tag{2.21}$$

Now P_i is the probability to belong to the ith *triangle* at time t. The factor of 3 reflects the fact that triangles have three neighbors rather than four. We shall solve the following problem given a gasket with 3^n triangles and potentials ϕ_0, ϕ_1, ϕ_2 at the boundary points. We seek the currents j_0, j_1, j_2 that flow out of the outer three vertices. Describing

$$\phi = \begin{bmatrix} \phi_0 \\ \phi_1 \\ \phi_2 \end{bmatrix}, \quad j \equiv \begin{bmatrix} j_0 \\ j_1 \\ j_2 \end{bmatrix},$$

we define the conductance matrix $\underline{\sigma}^n$ by

$$j = \underline{\sigma}^n \phi . \tag{2.22}$$

The C_3 point-group symmetry of the gasket dictates that $\underline{\sigma}^n$ has the structure

$$\underline{\sigma}^n = \begin{bmatrix} a_n & b_n & b_n \\ b_n & a_n & b_n \\ b_n & b_n & a_n \end{bmatrix} . \tag{2.23}$$

In steady state the rate of change of mass in the gasket must vanish, i.e., the sum of the currents must vanish. For the special case $\phi_0 = \phi_1 = \phi_2$, the currents are all equal by symmetry, and thus they all vanish. Then (2.23) gives

$$a_n = -2b_n . \tag{2.24}$$

In order to calculate j we shall now derive a recursion relation for a_n and solve it. To do so we consider an $(n+1)$-gasket (i.e., with 3^{n+1} triangles) which comprises three n-gaskets as shown in Fig. 2. We are now interested in the currents flowing into the vertices 00, 11, and 22 under the boundary conditions

$$\psi_1 = \begin{bmatrix} \phi_{00} \\ \phi_{11} \\ \phi_{22} \end{bmatrix} . \tag{2.25}$$

The calculation of σ^{n+1} is presented in Appendix A. The result is the recursion relation (obtained after setting $W = 1$ for convenience)

$$a_{n+1} = \frac{6a_n}{10 - 3a_n} = -2b_{n+1} \tag{2.26}$$

with $Y_n = 1/a_n$. Equation (2.26) reads

$$Y_{n+1} = \tfrac{5}{3} Y_n - \tfrac{1}{2} . \tag{2.27}$$

Denoting further $Z_n = Y_n - \tfrac{3}{4}$ we have

$$Z_{n+1} = \tfrac{5}{3} Z_n \tag{2.28}$$
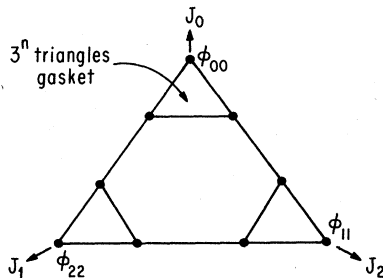
FIG. 2. A 3^{n+1}-gasket constructed from three 3^n-gaskets. ϕ_{00}, ϕ_{11}, and ϕ_{22} are the boundary potentials. j_0, j_1, and j_2 are the currents leaving the boundary points.

or

$$Z_n = (\tfrac{5}{3})^{n-1} Z_1 . \tag{2.29}$$

The recursion relation (2.22) therefore has the solution

$$a_n = [(\tfrac{5}{3})^{n-1} Z_1 + \tfrac{3}{4}]^{-1} \tag{2.30}$$

and in particular $a_1 = (Z_1 + \tfrac{3}{4})^{-1}$. It is easy to see however that the $(n=1)$-gasket (three sites) dictates $a_1 = -2$, $b_1 = 1$ from which $Z_1 = -\tfrac{5}{4}$. Reinserting W we finally find

$$a_n = \frac{4W}{3 - 3(\tfrac{5}{3})^n}, \quad b_n = -a_n/2 . \tag{2.31}$$

Equation (2.27) determines $\underline{\sigma}^n$ and we can now find the currents for any boundary conditions. In particular we want to compare with Sec. II B 1 and we pick

$$\underline{\phi} = \begin{bmatrix} \phi \\ 0 \\ 0 \end{bmatrix} . \tag{2.32}$$

The total current flowing out of the bottom vertices is calculated now from (2.22), (2.23), and (2.31) with the result

$$\hat{J}_n = \frac{4W\phi}{3(\tfrac{5}{3})^n - 3} . \tag{2.33}$$

For large n this simplifies to

$$\hat{J}_n = \phi \tfrac{4}{3} W (\tfrac{3}{5})^n . \tag{2.34}$$

We can now compare Eq. (2.34) to (2.21) and calculate K and θ. On the n-gasket $r_0 = 2^n$, i.e., we choose lattice spacing equal to unity. This choice is required to be consistent with (2.9), since there are precisely 3^n sites in a gasket whose edge r_0 measures 2^n lattice spacings. Thus

$$\phi K D (2 + \theta - D)(2^n)^{D - \theta - 2} = \phi \tfrac{4}{3} W (\tfrac{3}{5})^n . \tag{2.35}$$

From this θ is firstly obtained. Since

$$\tfrac{3}{5} = 2^{D - \theta - 2} \tag{2.36}$$

and D in the present case is $\ln 3 / \ln 2$, we find

$$\theta = \frac{\ln 5}{\ln 2} - 2 \tag{2.37}$$

in agreement with previous derivations of θ.[3,4] Using this in Eq. (2.35) we find

$$K = 4W/3D(2 + \theta - D) . \tag{2.38}$$

We therefore have no free parameter in Eq. (1.4) for the present case. The calculation of K for the general d-dimensional case is presented in Appendix A. The final result is

$$K = \frac{2Wd}{(d+1)D(2 + \theta - D)} . \tag{2.39}$$

C. Numerical tests of steady-state properties

We can test the predictions of Eqs. (2.18) and (2.20) directly by numerical simulations. Such tests are both il-
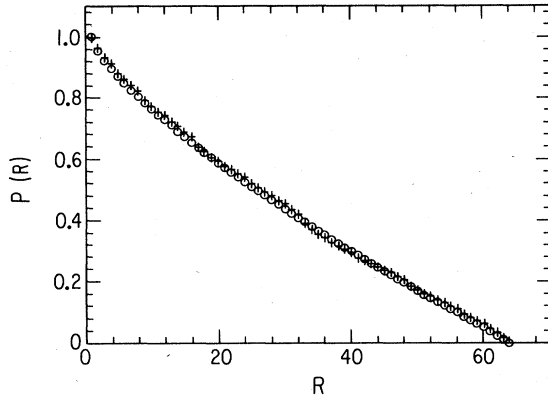
FIG. 3. The comparison of theory (O) and simulation (+) for the stationary probability distribution along the edge of a $d=2$, 3^6-gasket with boundary conditions (1,0,0).

FIG. 4. The four triangles that are explicitly considered in the renormalization-group theory.

luminating and important in view of the role that steady-state properties play in determining the parameters of Eq. (1.4). We have performed such simulations for $d=2,3,4$. In Fig. 3 we present the steady-state function $\hat{P}(r)$ along the edge of the $d=2$ Sierpiński gasket for boundary conditions as in Fig. 1. The circles represent the theoretical prediction Eq. (2.18), and the pluses symbolize the numerical value of $P(r)$. It appears that $\hat{P}(r)$ approximates $P(r)$ extremely well, except that there appears hardly noticeable steps in $P(r)$. It is our contention that these steps are in fact nonanalicities that repeat self-similarly on all length scales. Support of this contention will be supplied in Sec. IV in the context of the time dependent $P(r,t)$.

The results for $d=3$ and 4 are similar to $d=2$ except that the steps are more pronounced. In Sec. IV this tendency is also observed for $p(r,t)$.

III. RENORMALIZATION THEORY FOR THE GREEN'S FUNCTION FOR SIERPIŃSKI GASKETS

In order to support Eq. (1.4) beyond numerical simulations (which are presented in Sec. IV) we present here a renormalization-group theory for the Green's function $G_{i,j}(t)$ which is the probability to be at a triangle i at time t with initial conditions $P_i(0)=\delta_{ij}$, on a gasket of 3^n triangles. In the text we present the theory for the gasket embedded in two dimensions; Appendix B deals with the general case of gaskets in d dimensions.

We shall derive a recursion relation for $G_{i,j}^{(n)}(t)$ on the n-gasket, by relating it to $G_{\alpha i,\alpha j}^{(n-1)}(\beta t)$. In doing so we shall make full use of the coordinate systems shown in Fig. 1. Consider four neighboring triangles in the $(n-1)$-lattice, denoted by i, k, l, m (see Fig. 4). On the n-lattice each of these consists of three triangles which we denote as i_α, $i_\alpha=3i+\alpha$, etc., with $\alpha=0,1,2$ (Fig. 1). Defining $G_{ij}^{(n)}(E)$ to be the Laplace transform of $G_{ij}^{(t)}$, we see from Eq. (2.21) that generally speaking

$$\left[3-\frac{E}{W}\right]G_{i,j}^{(n)}(E)=\sum_k G_{k,j}^{(n)}(E)=\delta_{ij} \ , \qquad (3.1)$$
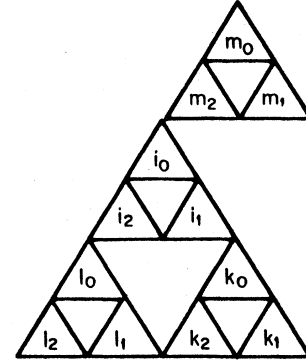
where the sum is over the neighbors k which are nearest to i. With initial conditions on the triangle j, which on the (n)-lattice is composed of j_0, j_1, j_2, we derive new equations for G_{i_α,j_s} which is defined by

$$G_{i_\alpha,j_s}=\sum_\beta G_{i_\alpha,j_\beta} \ , \qquad (3.2)$$

where the initial conditions are $P_{i_\beta}(0)=\delta_{i_\beta,j_\alpha}$. With the notation $\lambda\equiv 3-\epsilon$, $\epsilon=E/W$, and $\delta_{i_\alpha,j_s}=\sum_\beta\delta_{i_\alpha,j_\beta}$ these read (cf. Fig. 4)

$$\lambda G_{i_0,j_s}^{(n)}(\epsilon)=G_{i_1,j_s}^{(n)}(\epsilon)+G_{i_2,j_s}^{(n)}(\epsilon)+G_{m_2,j_s}^{(n)}+\delta_{i_0,j_s} \ , \qquad (3.3a)$$

$$\lambda G_{i_1,j_s}^{(n)}(\epsilon)=G_{i_0,j_s}^{(n)}(\epsilon)+G_{i_2,j_s}^{(n)}(\epsilon)+G_{k_0,j_s}^{(n)}(\epsilon)+\delta_{i_1,j_s} \ , \qquad (3.3b)$$

$$\lambda G_{i_2,j_s}^{(n)}(\epsilon)=G_{i_1,j_s}^{(n)}(\epsilon)+G_{i_0,j_s}^{(n)}(\epsilon)+G_{l_0,j_s}^{(n)}(\epsilon)+\delta_{i_2,j_s} \ , \qquad (3.3c)$$

$$\lambda G_{l_0,j_s}^{(n)}(\epsilon)=G_{i_2,j_s}^{(n)}(\epsilon)+G_{l_1,j_s}^{(n)}(\epsilon)+G_{l_2,j_s}^{(n)}(\epsilon)+\delta_{l_0,j_s} \ , \qquad (3.3d)$$

$$\lambda G_{k_0,j_s}^{(n)}(\epsilon)=G_{i_1,j_s}^{(n)}(\epsilon)+G_{k_1,j_s}^{(n)}(\epsilon)+G_{k_2,j_s}^{(n)}(\epsilon)+\delta_{k_0,j_s} \ , \qquad (3.3e)$$

$$\lambda G_{m_2,j_s}^{(n)}(\epsilon)=G_{i_0,j_s}^{(n)}(\epsilon)+G_{m_0,j_s}^{(n)}(\epsilon)+G_{m_1,j_s}^{(n)}(\epsilon)+\delta_{m_2,j_s} \ . \qquad (3.3f)$$

Next we multiply, say, Eq. (3.3c) by $(1+\lambda)$ and add it to Eq. (3.3d). We find

$$(\lambda^2+\lambda-1)G_{i_2,j_s}^{(n)}(\epsilon)=(1+\lambda)[G_{i_0,j_s}^{(n)}(\epsilon)+G_{i_1,j_s}^{(n)}(\epsilon)]$$
$$+G_{l_s,j_s}^{(n)}(\epsilon)+(1+\lambda)\delta_{i_2,j_s}+\delta_{l_0,j_s} \ , \qquad (3.4)$$

where

$$G_{l_s,j_s}^{(n)}(\epsilon)=\sum_\alpha G_{l_\alpha,j_s}^{(n)}(\epsilon) \ . \qquad (3.5)$$

Similarly we calculate

$$(\lambda^2+\lambda-1)G_{i_0,j_s}^{(n)}=(1+\lambda)[G_{i_1,j_s}^{(n)}(\epsilon)+G_{i_2,j_s}^{(n)}(\epsilon)]$$

$$+G_{m_s,j_s}^{(n)}+(1+\lambda)\delta_{i_0,j_s}+\delta_{m_2,j_s} \qquad (3.6)$$

and

$$(\lambda^2+\lambda+1)G_{i_1,j_s}^{(n)}(\epsilon)=(1+\lambda)[G_{i_0,j_s}^{(n)}(\epsilon)+G_{i_2,j_s}^{(n)}(\epsilon)]$$

$$+G_{k_s,j_s}^{(n)}(\epsilon)+(1+\lambda)\delta_{i_1,j_s}+\delta_{k_0,j_s} \ . $$

$$(3.7)$$

Adding up Eqs. (3.4), (3.6), and (3.7) we find

$$(\lambda^2-\lambda-3)G_{i_s,j_s}^{(n)}(\epsilon)=G_{i_s,j_s}^{(n)}(\epsilon)+G_{m_s,j_s}^{(n)}(\epsilon)$$

$$+G_{k_s,j_s}^{(n)}(\epsilon)+(1+\lambda)\delta_{i_s,j_s}$$

$$+\delta_{l_0,j_s}+\delta_{k_0,j_s}+\delta_{m_0,j_s} \ . \qquad (3.8)$$

We now denote

$$(3-\epsilon')=(\lambda^2-\lambda-3) \qquad (3.9)$$

and notice that $\delta_{i_s,j_s}=3\delta_{ij}$. The crucial step now is to compare Eq. (3.8) and (3.1) and see that the system (3.8) has the same structure as a sum of systems (3.1). Thus

$$G_{i_s,j_s}^{(n)}(\epsilon)=3(1+\lambda)G_{i,j}^{(n-1)}(\epsilon')+\sum_q G_{q,j}^{(n-1)}(\epsilon') \ , \qquad (3.10)$$

where q is nearest neighbor to i.

At this point we want to use Eq. (3.10) to compare with the diffusion-equation approach. The latter is expected to be applicable for i and j that are far apart. We then have

$$G_{q,j}^{(n-1)}(\epsilon)\simeq G_{i,j}^{(n-1)}(\epsilon) \qquad (3.11)$$

and

$$G_{i_\alpha,j_\beta}^{(n)}(\epsilon)\simeq G_{i_0,j_0}^{(n)}(\epsilon)\equiv G_{3i,3j}^{(n)}(\epsilon) \qquad (3.12)$$

in our coordinate system. Remembering that $\lambda=3-\epsilon$ we get finally

$$G_{3i,3j}^{(n)}(\epsilon)\simeq\left[\frac{5-\epsilon}{3}\right]G_{i,j}^{(n-1)}(5\epsilon-\epsilon^2) \ . \qquad (3.13)$$

On the infinite lattice, where boundary conditions can be neglected, we expect the Green's function to be the fixed-point function $G_{i,j}^*(\epsilon)$ of the recursion relation (3.13). Furthermore, since we are interested in long times we can consider the limit $\epsilon\rightarrow 0$ to find that Eq. (3.13) predicts that

$$G_{3i,3j}^*(t)=\tfrac{1}{3}G_{i,j}^*(t/5) \ . \qquad (3.14)$$

This result is valid for the embedding dimension $d=2$. The generalization to d dimensions is presented in Appendix B with the final result

$$G_{(d+1)i,(d+1)j}^*(t)=\frac{1}{d+1}G_{i,j}^*(t/d+3) \ . \qquad (3.15)$$

A. Comparison with the diffusion equation

We are now in a position to compare the predictions of Eq. (1.4) with the results for the Green's function (3.14) and (3.15). In particular it is important to check whether Eq. (1.5) is a solution to the fixed-point equations (3.14) and (3.15). To see that this is indeed the case pick, for example, $j=0$ (i.e., initial conditions at the top of the gasket). In two dimensions Eq. (3.14) reads

$$G_{3i}(t)=\tfrac{1}{3}G_i(t/5) \ . \qquad (3.16)$$

A solution of this equation is

$$G_i(t)=C_1\exp(-i^{\ln5/\ln3}/C_2t)/t^{\ln3/\ln5} \ . \qquad (3.17)$$

Of course this solution matches the initial conditions $G_i(t=0)=\delta_i$. Since for the gasket the distance from the top in the embedding space satisfies $r\propto i^{\ln2/\ln3}$ (cf. Fig. 1), Eq. (3.17) can be rewritten as

$$G(r,t)=C_3\exp(-r^{\ln5/\ln2}/C_4t)/t^{\ln3/\ln5} \ . \qquad (3.18)$$

In d dimensions, where $r\propto i^{\ln2/\ln(d+1)}$, Eq. (3.18) reads

$$G(r,t)=C_5\exp(-r^{\ln(d+3)/\ln2}/C_6t)t^{\ln(d+1)/\ln(d+3)} \ . $$

$$(3.19)$$

Remembering that the gaskets are characterized in d dimensions by [cf. Eqs. (A14) and (A15)]

$$D=\ln(d+1)/\ln2 \ , \qquad (3.20)$$

$$2+\theta=\ln(d+3)/\ln2 \ , \qquad (3.21)$$

we see that Eq. (1.5) agrees exactly with Eqs. (3.18) and (3.19) in two and in higher dimensions. We have to bear in mind, however, that Eq. (1.5) is only meant to be an envelope to a possibly very singular function $G(r,t)$. Indeed, Eq. (3.15) relates only points i,j to points $(d+1)^n i,(d+1)^n j$. In the numerical simulations shown below we shall find that $P(r,t)$ is very far from being smooth and appears to have discontinuities on all length scales. These discontinuities have self-similar appearance as discussed at some length in Sec. IV. As will be shown, however, Eq. (1.5) provides an excellent envelope approximation to $P(r,t)$.

It is slightly more difficult to test the predictions of Eq. (3.15) for $j\neq0$ against (1.5) because it is harder to transform from i to r in the general case, and (1.5) is valid in r space. For this reason we test Eq. (3.15) for general i,j numerically in Sec. IV.

IV. NUMERICAL SIMULATIONS

Here we present typical comparisons of $\hat{P}(r,t)$ to $P(r,t)$ obtained numerically for Sierpiński gaskets at $d=2,3,4$. Figure 5 shows $P(r,t)$ versus r along the edge of the $d=2$ gasket with δ-function initial conditions at the top, at two different times. $\hat{P}(r,t)$ is computed from Eq. (1.5). The quality of the envelope approximation is apparent. The same quality pertains to $d=3,4$ as shown in Figs. 6 and 7. We reiterate that no free parameters exist in Eq. (1.5).

Similar to Fig. 3, $P(r,t)$ seems to exhibit steps or discontinuities that are already apparent in Fig. 5 but be-
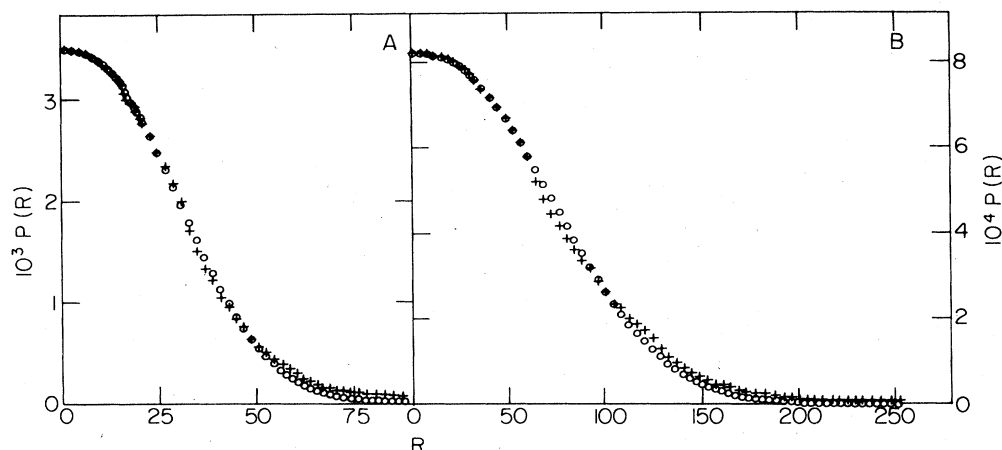
FIG. 5. Typical plots of $p(r,t)$ vs r along the edge of a $d=2$, 3^8-gasket with δ-function initial conditions at the top and $W=0.25$. (a) $t=3000$ and r in dimensionless units. Numerical simulations plotted with crosses, analytical predictions with open circles. (b) $t=25\,000$, otherwise identical to (a).

come more pronounced at $d=3,4$ (Figs. 6 and 7). These discontinuities are in fact self-similar and related to the underlying self-similarity of the fractal object. To see this we present plots of $\log_{10}[P(r,t)/P(0,t)]$ versus $-r^{2+\theta}/t$ for $d=2$, 3, 4 in Figs. 8(a), 9(a), and 10(a). If it were not for the nonanalyticity, we would have expected to see here straight lines [cf. Eq. (1.5)]. Figures 8(b)—8(d), 9(b)—9(d), and 10(b)—10(d) show blowups of Figs. 8(a), 9(a), and

FIG. 6. Same as Fig. 5, but for a $d=3$, 4^6-gasket. (a) $t=1000$, $W=\frac{1}{6}$. (b) $t=2000$. (c) $t=3000$. Notice the discontinuities in the numerical $P(r,t)$.
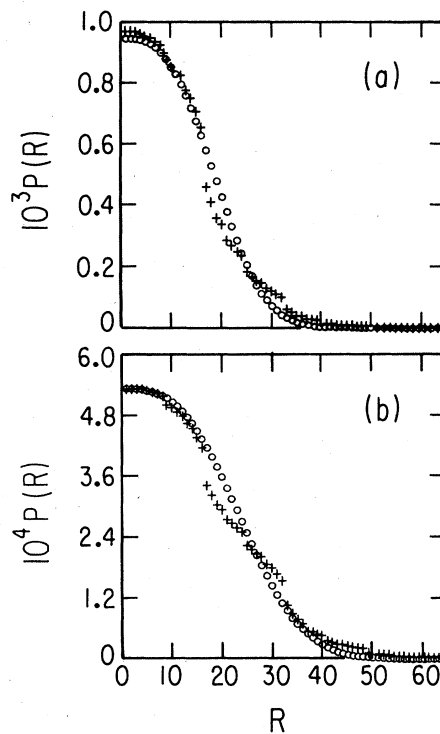
FIG. 7. Same as Fig. 5, but for a $d=4$, 5^6-gasket. (a) $t=3500$, $W=\frac{1}{8}$. (b) $t=7000$. The discontinuities in $P(r,t)$ become even more apparent.
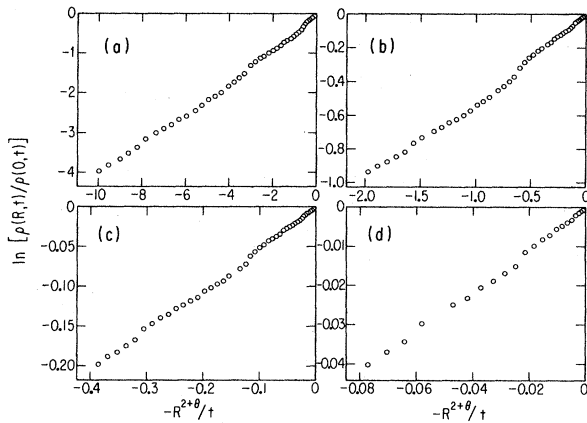
FIG. 8. Successive blowups in $\log_{10}[P(r,t)/P(r,0)]$ vs $x \equiv -R^{2+\theta}/t$ for a $d=2$, 3^8-gasket to display the self-similarity of the discontinuities. (a) $0>x>-10$. (b) $0>x>-2$. (c) $0>x>-\frac{2}{5}$. (d) $0>x>-\frac{2}{25}$.

10(a), respectively. We see that down to the smallest available scale the structure appears self-similar. Notice that in all cases r is halved in each blowup. Accordingly $r^{2+\theta}$ is scaled down by a factor of $(d+3)$ [cf. Eq. (A15)].

So far we compared theory and simulation along the edge of the gasket. The scaling prediction (3.15) can be tested for arbitrary sites as well. Figure 11 displays $\ln G(0,j,t)$ versus $\ln j$ for $d=2$ where $t=5^n\times40$ and $j=3^n j_0$, $n=1,2,\ldots,6$. Curves for six different j_0 values which are picked from internal points in the gasket are shown. According to Eq. (3.15) a slope of -1 is anticipated for all these curves. Such a line is drawn for comparison. All six curves support the scaling prediction very closely.
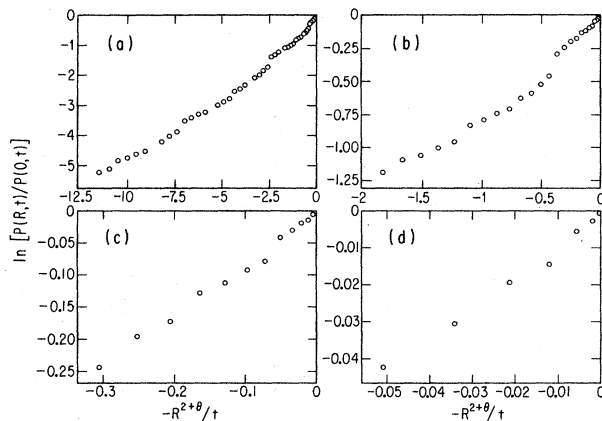
FIG. 9. Same as Fig. 8 but for a $d=3$, 4^6-gasket. (a) $0>x>-12$. (b) $0>x>-2$. (c) $0>x>-\frac{2}{6}$. (d) $0>x>-\frac{1}{18}$.
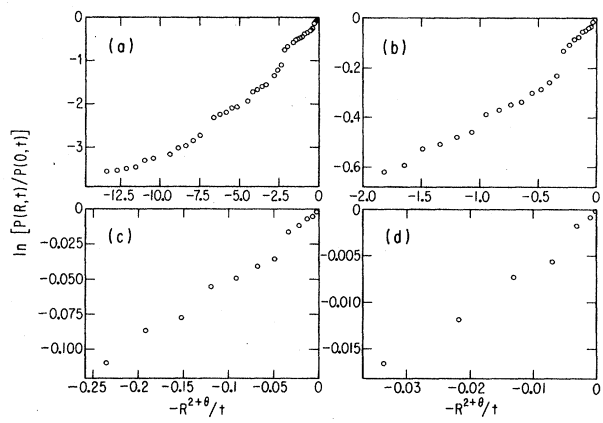
FIG. 10. Same as Fig. 8 but for a $d=4$, 5^6-gasket. (a) $0>x>-14$. (b) $0>x>-2$. (c) $0>x>-\frac{2}{7}$. (d) $0>x>-\frac{2}{49}$.

V. DISCUSSION

The central statements of this paper are as follows.

(i) For a random walk on a fractal we do not expect the probability distribution $P(r,t)$ to be a smooth function of r. For self-similar fractals we expect $P(r,t)$ to have discontinuities self-similarly on all length scales (cf. Figs. 8—10).

(ii) Notwithstanding these discontinuities, we can approximate $P(r,t)$ very well with an envelope function $\hat{P}(r,t)$ which solves a diffusion equation which is our suggestion for the generalization of Fickian diffusion to fractal lattices.

(iii) The anomaly in diffusion is characterized by the exponent θ which is the same exponent that governs the scaling of the conductivity. It is our conjecture therefore that in all cases where the conductivity scales as a power law, a diffusion equation of the form (1.5) should yield a good envelope description of $P(r,t)$. One should stress that an experiment to measure the scaling of conductivity is an equilibrium experiment, which seems considerably easier than any dynamical experiment.

As a final note we comment that the simulations at
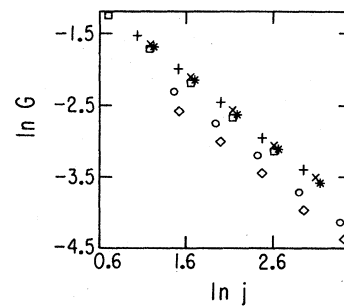
FIG. 11. Numerical test of the scaling prediction Eq. (3.15). See text for explanation. The notation is $\square$, $j_0=5$; $+$, $j_0=11$; $\times$, $j_0=15$; $\ast$, $J_0=11$; $\circ$, $j_0=29$; $\Diamond$, $J_0=33$.

$d=2,3,4$ showed that the entire function $P(r,t)$ oscillated periodically in time with period $d+3$ about the envelope $\hat{P}(r,t)$.

We found that these oscillations increase in amplitude with increasing d just as the discontinuities in space do. In this sense $\hat{P}(r,t)$ is the smoothed out version of $P(r,t)$ both in space and time.

APPENDIX A: DETERMINATION OF K FOR GASKETS IN d DIMENSIONS

Here we present the general case of d dimensions. The case $d=2$ discussed in Sec. II can be easily inferred.

The d-dimensional n-gasket has $d+1$ boundary sites. We can therefore fix $d+1$ potentials $(\Psi_0, \Psi_1, \ldots, \Psi_{d+1})$. The $(d+1) \times (d+1)$ matrix $\underline{\sigma}^n$ relates the currents to these potentials as in Eq. (2.22). The same arguments that followed Eq. (2.22) imply now that an $\underline{\sigma}^n$ has the form

$$\underline{\sigma}^n = \begin{bmatrix} a_n & -\dfrac{a_n}{d} & \cdots & -\dfrac{a_n}{d} \\ -\dfrac{a_n}{d} & a_n & \dfrac{a_n}{d} & \cdots \\ \cdots & \cdots & \cdots & \cdots \\ \cdots & \cdots & \cdots & a_n \end{bmatrix} . \quad \text{(A1)}$$

We want to determine a_n by calculating $\underline{\sigma}^{n+1}$ which pertains to $d+1$ n-gaskets put together, which constitute the $(n+1)$-gasket. As an example we show in Fig. 12 the situation for $d=3$. (We reiterate that every vertex in the figure denotes actually a hypertriangle rather than a site.) Since $\underline{\sigma}^n$ is determined by only one parameter, we can
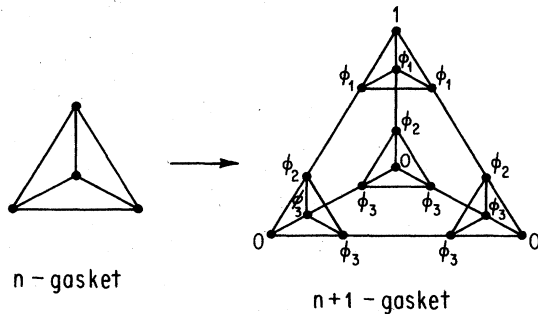
FIG. 12. The boundary conditions and notation used for the calculation of the currents are shown for $d=3$ as an example. Notice that there exists only three independent values of ϕ in any dimension d.

choose a special arrangement of boundary potentials like the one shown in Fig. 12. The potential is 1 at the "top" and zero at d bottom sides. By symmetry (see Fig. 12) there are only three unknown potentials, ϕ_1, ϕ_2, and ϕ_3. Note that this remains true for any d with these boundary conditions. Taking now the conductivity w as unity (we reinsert w at the end), we see that in the steady-state Kirchhoff's laws imply:

$$a_n \phi_1 - \frac{a_n}{d}[1+(d-1)\phi_1] = \phi_1 - \phi_2 , \quad \text{(A2a)}$$

$$a_n \phi_2 - \frac{a_n}{d}(d-1)\phi_3 = \phi_2 - \phi_1 , \quad \text{(A2b)}$$

$$a_n \phi_3 - \frac{a_n}{d}[\phi_2 + (d-2)\phi_3] = 0 . \quad \text{(A2c)}$$

From these equations we find

$$\phi_1 = \frac{a_n - d\phi_2}{a_n - d} , \quad \text{(A3)}$$

$$\phi_2 = 2da_n[(d-a_n)(a_n d + a_n - 2d) + 2d^2]^{-1} . \quad \text{(A4)}$$

Now let J be the current flowing into the top vertex (this of course equals the sum of currents flowing out of all "bottom" vortices):

$$J = a_n 1 - \frac{a_n}{d}(\phi_1 + \phi_1 + \cdots + \phi_1) = a_n(1 - \phi_1) . \quad \text{(A5)}$$

Using (A3) and rearranging we find

$$J = \frac{a_n d(d+1)}{d(3+d) - a_n(d+1)} . \quad \text{(A6)}$$

Now the matrix $\underline{\sigma}^{n+1}$ pertains to Fig. 12 looked at as one single hypertriangle. Therefore

$$J = a_{n+1} \times 1 - \frac{a_{n+1}}{d}(0+0+\cdots+0) = a_{n+1} . \quad \text{(A7)}$$

We thus have the desired recursion relation

$$a_{n+1} = \frac{a_n d(d+1)}{d(3+d) - a_n(d+1)} . \quad \text{(A8)}$$

Repeating now the tricks of Sec. II for this general case we find

$$a_n = \frac{2dw}{d+1 - \left[\dfrac{d+3}{d+1}\right]^n (d+1)} , \quad \text{(A9)}$$

where W has been reinserted. In deriving (A9), $a_1 = -d$ has been used. This follows since (for $W=1$ on the 1-gasket)

$$j_0 = \sum_{i=1}^{d} (\phi_1 - \phi_0) = -d\phi_0 + \sum_{i=1}^{d} \phi_i .$$

Since we now have σ^n we can calculate the currents under the boundary potential vector $(\phi, 0, 0, \ldots, 0)$. The total current flowing into the bottom sites (equal to the current flowing out of the top site) is then

$$\hat{J}_n = \frac{2dw\phi}{(d+1)\left[\dfrac{d+3}{d+1}\right]^n - (d+1)} \qquad (A10)$$

or for large n

$$\hat{J}_n = \frac{2dw\phi}{(d+1)\left[\dfrac{d+3}{d+1}\right]^n} . \qquad (A11)$$

$\hat{J}_n$ is the total radial current flowing through the gasket. As before (Sec. II) we have to match this equation with Eq. (2.20). Since on the n-gasket $r_0 = 2^n$ in all embedding dimensions, we have now

$$\phi KD(2+\theta-D)(2^n)^{\theta-D-2}$$
$$= 2dw\phi/(d+1)[(d+3)/d+1] , \qquad (A12)$$

where

$$D - \theta - 2 = \ln[(d+1)/d+3]/\ln 2 . \qquad (A13)$$

But since

$$D = \ln(d+1)/\ln 2 \qquad (A14)$$

we find

$$\theta = \ln(d+3)/\ln 2 - 2 . \qquad (A15)$$

Further, (A12) implies that

$$K = 2dW/D(d+1)(2+\theta-D) . \qquad (A16)$$

Equation (A16) is our main result here. Although the result (A15) is known, we feel this particular derivation underlines the equivalence of anomalous diffusion and the anomalous scaling of the resistance (see Sec. V). Having calculated θ and K we can now compare the predictions of Eq. (1.4) to numerical simulations in all dimensions d.

APPENDIX B: RENORMALIZATION GROUP IN d DIMENSIONS

The coordinate system appropriate to the d-dimensional Sierpeński gasket is a natural generalization of that used for $d=2$. On the n-gasket, which comprises $(d+1)^n$ hypertriangles, the latter are labeled by $i = \sum_{k=0}^{n-1} a_K(d+1)^K$, $a_K = 0, 1, \ldots, d$. The basic repeating unit of the gasket is a hypertriangle of $d+1$ sides (bonds). A site is the common vertex of two neighboring hypertriangles. The vertex of such a hypertriangle has d bonds leaving it: thus a site has $2d$ bonds leaving it, i.e., has $2d$ nearest neighbors. The site diffusion equation is

$$\dot{Q}_p = W\left[\sum_q Q_q - 2dQ_p\right] , \qquad (B1)$$

where $\sum_q$ is over the $2d$ nearest neighbors of site p, and W is the conductance of a bond or the hopping frequency.

Consider the equations (B1) for each of the $(d+1)$ sites q belonging to the hypertriangle labeled i. Their sum is

$$\frac{1}{W}\sum_{q\in i}\dot{Q}_q = d\sum_{q\in i}Q_q + \sum_j \sum_{\substack{q \\ (q\in j, \\ q\notin i)}} Q_q - 2d\sum_{q\in i}Q_q . \qquad (B2)$$

The prefactor in the first term on the right-hand side of (B2) is d other than $(d+1)$ since one site in hypertriangle i is omitted for each member of the sum of equations (B1). The second term is a sum over nearest-neighbor hypertriangles to i, called j.

Rearranging terms in (B2) gives

$$\frac{1}{W}\dot{p}_i = (d-1)p_i + \sum_j p_j - 2dp_i , \qquad (B3)$$

where p_i is defined as the sum of the amplitudes Q_i over all $(d+1)$ vertices of i. We define p_i as the probability to be at hypertriangle i. Equation (B3) is

$$\dot{p}_i = W\left[\sum_j p_j - (d+1)p_i\right] . \qquad (B4)$$

We have transformed Eq. (B1) for sites into a hypertriangle diffusion equation with coordination number $(d+1)$ rather than $2d$. The sum runs over the $(d+1)$ neighboring hypertriangles.

To analyze the Green's function, consider an $(n-1)$-gasket embedded in d dimensions. Consider the $(d+1)$ hypertriangles $i, i+1, \ldots, i+d$ which comprise a larger hypertriangle of the next size up. Let k label the remaining nearest neighbor of i.

Now consider the n-gasket obtained by converting each of these hypertriangles into $(d+1)$ hypertriangles which we label i_α, $\alpha = 0, 1, \ldots, d$ (see Fig. 13 where this is illustrated for $d=2$).

The Green's function $G_{ij}^n(E)$ on the n-gasket is defined by

$$\left[(d+1) - \frac{E}{W}\right]G_{ij}^n(E) = \sum_k G_{kj}^n(E) + \delta_{ij} \qquad (B5)$$

which results from Laplace transformation of (B4) with appropriate initial conditions. We employ notation where subscript s denotes summation (e.g., $G_{i_\alpha, j_s}^n \equiv \sum_{\beta=0}^d G_{i_\alpha, j_\beta}^n$) and $\epsilon \equiv E/W$, $\lambda\epsilon \equiv d+1-\epsilon$. The equations (B5) for i_0 and each of its nearest neighbors are then (see Fig. 13)

$$\lambda G_{i_0, j_s}^n(\epsilon) = \sum_{\alpha=1}^d G_{i_\alpha, j_s}^n(\epsilon) + G_{k_d, j_s}^n(\epsilon) + \delta_{i_0, j_s} , \qquad (B6)$$

$$\lambda G_{k_d, j_s}^n(\epsilon) = \sum_{\alpha=0}^{d-1} G_{k_\alpha, j_s}^n + G_{i_0, j_s}^n + \delta_{k_d, j_s} , \qquad (B7)$$
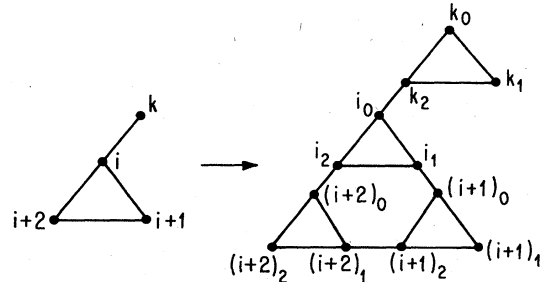
FIG. 13. The notation used for the renormalization-group calculation in d dimensions is shown for $d=2$ as an example.

$$\lambda G^n_{i_p, j_s} = \sum_{\substack{\alpha=0 \\ \alpha \neq p}}^{d} G^n_{i_\alpha, j_s} + G^n_{(i+p)_0, j_s} + \delta_{i_p, j_s}, \quad p = 1, d \qquad \text{(B8)}$$

$$\lambda G_{(i+p)_0, j_s} = \sum_{\alpha=1}^{d} G^n_{(i+p)_\alpha, j_s} + G^n_{i_p, j_s} + \delta_{(i+p)_0, j_s},$$
$$p = 1, \ldots, d . \qquad \text{(B9)}$$

Each equation has been summed over the j in a large hypertriangle. Note that i_α and $(i+\alpha)_0$ are neighbors as are i_0 and k_d (Fig. 13). Multiplying (B8) by $(1+\lambda)$ and adding to (B9) we obtain

$$(\lambda^2 + \lambda + 1) G^n_{i_p, j_s} = (1 + \lambda) \sum_{\substack{\alpha=0 \\ (\alpha \neq p)}}^{d} G^n_{i_\alpha, j_s} + \sum_{\alpha=0}^{d} G^n_{(i+p)_\alpha, j_s}$$
$$+ (1+\lambda) \delta_{i_p, j_s} + \delta_{(i+p)_0, j_s}, \quad p = 1, \ldots, d . \qquad \text{(B10)}$$

Similarly from (B6) and (B7) we have

$$(\lambda^2 + \lambda + 1) G^n_{i_0, j_s} = (1 + \lambda) \sum_{\alpha=1}^{d} G^n_{i_\alpha, j_s} + \sum_{\alpha=0}^{d} G^n_{k_\alpha, j_s}$$
$$+ (1+\lambda) \delta_{i_0, j_s} + \delta_{k_d, j_s} . \qquad \text{(B11)}$$

Summing Eq. (B10) over $p \sum_{p=1}^{d}$ and adding to (B11) gives

$$[\lambda^2 + (1-d)\lambda - (d+1)] G^n_{i_s, j_s}$$
$$= \sum_{p=1}^{d} G^n_{(i+p)_s, j_s} + G^n_{k_s, j_s} + (1+\lambda) \delta_{i_s, j_s}$$
$$+ \sum_{q=1}^{d} \delta_{(i+p)_0, j_s} + \delta_{k_d, j_s} . \qquad \text{(B12)}$$

Note that $\delta_{i_s, j_s} = (d+1)\delta_{ij}$, $\delta_{(1+p)_0, j_s} = \delta_{i+p, j}$, and $\delta_{K_d, j_s} + \delta_{Kj}$. Defining $\lambda^1 \equiv \lambda^2 + (1-d)\lambda - (d+1)$, and defining ϵ' by $\lambda' \equiv (d+1) - \epsilon'$ we have

$$\epsilon' = (d+3)\epsilon - \epsilon^2 \qquad \text{(B13)}$$

using $\lambda \equiv (d+1) - \epsilon$. Thus (B12) becomes

$$[(d+1) - \epsilon'] G^n_{i_s, j_s}(\epsilon)$$
$$= \sum_{p=1}^{d} G^n_{(i+p)_s, j_s} + G^n_{K_s, j_s} + (d+1)(1+\lambda)\delta_{ij}$$
$$+ \sum_{p=1}^{d} \delta_{1+p, j} + \delta_{Kj} . \qquad \text{(B14)}$$

Noting that $(i+p)$, $p = 1, \ldots, d$, and k are the nearest neighbors to i on the $(n-1)$-lattice, we see that the system of equations (B14) for $G^n_{i_s, j_s}(\epsilon)$ has the same structure as a sum of systems of equations for $G^{(n-1)}_{ij}(\epsilon')$:

$$G^n_{i_s, j_s}(\epsilon) = (d+1)(1+\lambda) G^{n-1}_{ij}(\epsilon') + \sum_q G^{n-1}_{qj}(\epsilon') ,$$
$$\text{(B15)}$$

where $\sum_q$ is a sum over the $(d+1)$ nearest neighbors to i on the $(n-1)$-lattice. As for $d=2$ (Sec. III) we consider i, j far apart when $G_{qj} \simeq G_{ij}$ and $G_{i_\alpha, j_\beta} \simeq G_{i_0, j_0} = G_{(d+1)i, (d+1)j}$ so (B15) becomes

$$(d+1)^2 G^n_{(d+1)i, (d+1)j}(\epsilon) = (d+1)(2+\lambda) G^{n-1}_{ij}(\epsilon') .$$
$$\text{(B16)}$$

The fixed-point function thus obeys

$$G^*_{(d+1)i, (d+1)j}(\epsilon) = \left[\frac{d+3-\epsilon}{d+1} \right] G^*_{ij}((d+3)\epsilon - \epsilon^2) ,$$
$$\text{(B17)}$$

where we have substituted ϵ' [from (B13)] and λ. Taking the $\epsilon \to 0$ limit of (B17) and inverse Laplace transforming we have for long times

$$G^*_{(d+1)i, (d+1)j} = \frac{1}{d+1} G^*_{ij}(t/(d+3)) . \qquad \text{(B18)}$$

---

*Present and permanent address: Department of Chemical Physics, The Weizmann Institute of Science, 76100 Rehovot, Israel.

[1]Y. Gefen, A. Aharony, and S. Alexander, Phys. Rev. Lett. **50**, 77 (1983).

[2]E. Domany, S. Alexander, D. Bensimon, and L. P. Kadanoff, Phys. Rev. B **28**, 3110 (1983).

[3]S. Alexander and R. Orbach, J. Phys. (Paris) Lett. **43**, 2625 (1982).

[4]Y. Gefen, A. Aharony, B. B. Mandelbrot, and S. Kirkpatrick, Phys. Rev. Lett. **47**, 1771 (1981).

[5]R. Lenormand and C. Zarcone (unpublished).

[6]F. Leyvraz and H. E. Stanley, Phys. Rev. Lett. **51**, 2048 (1983).

[7]A short presentation of the ideas is found in B. O'Shaughnessy and I. Procaccia, Phys. Rev. Lett. **54**, 455 (1905).

[8]R. Rammal and G. Toulouse, J. Phys. (Paris) Lett. **44**, L13 (1983).

[9]B. B. Mandelbrot, *The Fractal Geometry of Nature* (Freeman, San Francisco, 1983).

[10]J. R. Banavar and J. Willemsen, Phys. Rev. B **30**, 6778 (1984).

[11]S. Wilke, Y. Gefen, V. Ilkovic, A. Aharony, and D. Stauffer, J. Phys. A **17**, 647 (1984).

[12]R. A. Guyer, Phys. Rev. A **29**, 2751 (1984).

[13]J. C. Angles d'Auriac, A. Benoit, and R. Rammal, J. Phys. A **16**, 4039 (1983).